NMRlipids IV: Headgroup & glycerol backbone structures, and cation binding in bilayers with PE and PG lipids

O. H. Samuli Ollila[1, 2, *]

[1] *Institute of Organic Chemistry and Biochemistry, Academy of Sciences of the Czech Republic, Prague 6, Czech Republic*
[2] *Institute of Biotechnology, University of Helsinki*

(Dated: October 29, 2019)

Primarily measured but also simulated NMR order parameters will be collected also for other than phophatidylcholine (these are discussed in NMRlipids I) headgroup. The information will be used to understand structural differences between different lipid molecules in bilayers.

INTRODUCTION

PE and PG lipids are most common lipids in bacteria [1]. Zwitterionic PE is the second most abundant glycerophospholipid in eukaryotic cells and has been related to the diseases [2–4]. Anionic PG lipids are less abundant, but is also proposed to be fundamental for terrestrial life [5]. PE and PG affect membrane protein functionality [6] and bind to various proteins [7]. PE headgroup is also prone for negative membrane curvature and causes membrane fusion [**?**]. Therefore, the PE and PG headgroup structures play probably essential roles in many biological processes.

Structural details of lipid headgroups are mainly studied using NMR experiments, which suggest that the glycerol backbone structures are largely similar irrespectively of the headroup [8], glycerol backbone and headgroup structure and behaviour are similar in model membranes and in bacteria [8–10], and the headgroup structures are similar in PC, PE and PG lipids, while headgroup is more rigid in PS lipids [11, 12]. Some attempts to resolve conformational ensembles from NMR for PC lipids have been made, but lesser extend for other lipids [**?**]. Classical molecular dynamics simulations could potentially give such ensembles and therefore enable the detailed studies of lipid headgroup behaviour in complex biomolecular systems, but current force fields are not accurate enough to reproduce the correct conformational ensembles for PC and PS headgroups [13, 14]. Several MD simulations of PE and PG lipids have been published especially in the context of modeling inner membrane of Gram-negative bacteria [**?**], but glycerol backbone and headgroup structures have not been evaluated against experiments.

Besides the structure, also ion binding may regulate biophysical activity of especially negatively charged lipid headgroups [**?**]. Monovalent cation (except Lithium) binding to zwitterionic PC headgroups is very weak, while multivalent ion binding is stronger but still weak [**?**]. The ion binding affinity data for PE is more scarce [**?**], but large differences to PC would be surprising. Negatively charged lipids are suggested to bear same cation binding constants than zwitterionic lipids, but the amount of bound ions to negatively charged membranes would still be larger because the concentration of cations in the vicinity of membranes would be higher [10]. On the other hand, anionic PS lipids are proposed chelate with calcium ions [**?**]. In simulations, the cation binding affinity to PC and PS membranes is typically overestimated [14, 15], which can be improved by applying the ECC to the partial charges of the force fields [16, 17].

Here, we use open collaboration and order parameters of glycerol backbone and headgroup to evaluate the accuracy of PE and PG heagroup structures, and the cation binding affinity to anionic membranes containing PG lipids in the current MD simulation force fields. The force field giving the best description for glycerol backbone and headgroup structures of PC, PS, PG and PE headgroups (CHARMM36) reproduces the essential differences in order parameters between these headgroups, and therefore enables the analysis of structural differences between the headgroups.

METHODS

Experimental C–H bond order parameters

The headgroup and glycerol backbone C–H bond order parameter magnitudes and signs of POPE and POPG were determined by measuring the chemical-shift resolved dipolar splittings with a R-type Proton Detected Local Field (R-PDLF) experiment [18] and S-DROSS experiments [19] using natural abundance ^{13}C solid state NMR spectroscopy as described previously [20, 21]. POPE and POPG powder were purchased from Avanti polar lipids. The NMR experiments were identical to our previous work [14]. **1.Is this enough and correct, or should we repeat some methods from the NMRlipidsIVps paper?**

Molecular dynamics simulations

Molecular dynamics simulation data were collected using the Open Collaboration method [13], with the NMRlipids Project blog (`nmrlipids.blogspot.fi`) and GitHub repository (`github.com/NMRlipids/NMRlipidsIVotherHGs`) as the communication platforms. The simulated systems of pure PE and PG bilayers without additional ions are listed in Tables I and II, and lipid mixtures with additional ions in Table III. Further simulation details are given in the SI, and the simulation data are indexed in a searchable database available at

www.nmrlipids.fi, and in the NMRlipids/MATCH repository (github.com/NMRlipids/MATCH).

The C–H bond order parameters were calculated directly from the carbon and hydrogen positions using the definition

$$S_{\mathrm{CH}} = \frac{1}{2}\langle 3\cos^2\theta - 1\rangle, \tag{1}$$

where θ is the angle between the C–H bond and the membrane normal (taken to align with z, with bilayer periodicity in the xy-plane). Angular brackets denote average over all sampled configurations. The order parameters were first calculated averaging over time separately for each lipid in the system. The average and the standard error of the mean were then calculated over different lipids. Python programs that use the MDAnalysis library [22, 23] used for all atom simulations is available in Ref. 24 (scripts/calcOrderParameters.py). For united atom simulations, the trajectories with hydrogens having ideal geometry were constructed first using either buildH program [25] or (scratch/opAAUA_prod.py) in Ref. 24, and the order parameters were then calculated from these trajectories. This approach has been tested against trajectories with explicit hydrogens and the deviations in order parameters are small [25, 26].

2.BuildH program is now cited with a direct link to the GitHub repo. I think that a release to Zenodo would be nice in the final publication.

3.Maybe we should also shortly discuss here about the reasons for slight dependence of order parameter values on the method used to reconstruct hydrogens?

The ion number density profiles were calculated using the gmx density tool of the Gromacs sofware package [27].

TABLE I: List of MD simulations with PE lipids.

lipid/counter-ions	force field for lipids / ions	NaCl (M)	[a]N_l	[b]N_w	[c]N_c	[d]T (K)	[e]t_{sim}(ns)	[f]t_{anal} (ns)	[g]files
POPE	CHARMM36 [**?**]	0	144	5760	0	310	500	400	[28]
POPE	CHARMM36 [**?**]	0	500	25000	0	310	500	100	[29]
POPE	CHARMM36 [**?**]	0.11	500	25000	50	310	500	100	[30]
POPE	CHARMM36ua [**?**]	0	336	15254	0	310	2×200	2×100	[31]
DPPE	Slipids [32]	0	288	9386	0	336	200	100	[33]
POPE	Slipids [32**?**]	0	336	?	0	310	2×200	2×100	[34]
POPE	Slipids [**?**]	0	500	25000	0	310	500	100	[35]
POPE	Slipids [**?**] 4.	0.11	500	25000	50	310	500	100	[36]
DPPE	GROMOS-CKP [**?**]	0	128	3655	0	342	2×500	2×400	[37]
POPE	GROMOS-CKP [**?**]	0	128	3552	0	313	2×500	2×400	[38]
POPE	GROMOS-CKP [**?**]	0	500	25000	0	310	500	100	[39]
POPE	GROMOS-CKP [**?**]	0.11	500	25000	50	310	500	100	[40]
DOPE	GROMOS-CKP [**?**]	0	128	4789	0	271	2×500	2×400	[41]
POPE	GROMOS 43A1-S3 [**?**]	0	128	3552	0	313	2×200	2×100	[42]
POPE	OPLS-UA vdW on H [**?**]	0	128	3328	0	303	2×200	2×100	[43]
POPE	OPLS-UA [**?**]	0	128	3328	0	303	2×200	2×100	[44]
POPE	Berger-Vries [**?**]	0	128	3552	0	303	2×200	2×100	[45]
POPE	Berger-largeH [**?**]	0	128	3552	0	303	2×200	2×100	[46]
DOPE	Berger-Vries [**?**]	0	128	4789	0	271	2×200	2×100	[47]
DOPE	Berger-largeH [**?**]	0	128	4789	0	271	2×300	2×100	[48]
POPE	LIPID17 [**?**]	0	500	25000	50	310	500	100	[49]
POPE	LIPID17 [**?**]	0.11	500	25000	50	310	500	100	[50]

[a]Number of lipid molecules with largest mole fraction
[b]Number of water molecules
[c]Number of additional cations
[d]Simulation temperature
[e]Total simulation time
[f]Time used for analysis
[g]Reference for simulation files

5.We need citations for the force fields.

TABLE II: List of MD simulations with PG lipids.

lipid/counter-ions	force field for lipids / ions	NaCl (M)	[a]N_l	[b]N_w	[c]N_c	[d]T (K)	[e]t_{sim}(ns)	[f]t_{anal} (ns)	[g]files
POPG/K^+	CHARMM36 [**?**] 6.	0	118	4110	0	298	100	100	[51]
POPG	CHARMM36 [**?**]	0.11	500	25000	49	310	500	100	[52]
POPG	CHARMM36 [**?**]	0	500	25000	0	310	500	100	[53]
POPG/Na^+	Slipids [54]	0	288	10664	0	298	250	100	[55]
DPPG/Na^+	Slipids [54]	0	288	11232	0	314	200	100	[56]
DPPG/Na^+	Slipids [54]	0	288	11232	0	298	400	100	[57]
POPG	Slipids [**?**] 7.	0	500	25000	0	310	500	100	[58]
POPG	Slipids [**?**] 8.	0.11	500	25000	49	310	500	100	[59]
POPG	LIPID17 [**?**]	0	500	25000	0	310	500	100	[60]
POPG	LIPID17 [**?**]	0.11	500	25000	49	310	500	100	[61]
POPG	GROMOS-CKP [**?**]	0	500	25000	0	310	500	100	[62]
POPG	GROMOS-CKP [**?**]	0.11	500	25000	49	310	500	100	[63]

[a]Number of lipid molecules with largest mole fraction
[b]Number of water molecules
[c]Number of additional cations
[d]Simulation temperature
[e]Total simulation time
[f]Time used for analysis
[g]Reference for simulation files

9.We need citations for the force fields.

TABLE III: List of MD simulations with PE and PG lipids mixed with PC.

lipid/counter-ions	force field for lipids / ions	NaCl (M)	$CaCl_2$ (M)	[a]N_l	[b]N_w	[c]N_c	[d]T (K)	[e]t_{sim}(ns)	[f]t_{anal} (ns)	[g]files
POPC	CHARMM36 [**?**]	0.11	0	500	25000	48	310	500	100	[64]
POPC:POPG (7:3)	CHARMM36 [**?**]	0.11	0	350	?	?	310	500	100	[65]
POPC:POPG (1:1)/K^+	CHARMM36 [**?**]	0	0	250:250	18158	0	298	200	200	[66]
POPC:POPG (1:1)	CHARMM36 [**?**]	0	0.34 10.	250:250	20798	128	298	200	200	[67]
POPC:POPG (1:1)	CHARMM36 [**?**]	0	1.36 11.	250:250	18114	445	298	200	200	[68]
POPC:POPG (4:1)/K^+	CHARMM36 [**?**]	0	0	400:100	18664	0	298	200	200	[69]
POPC:POPG (4:1)/K^+	CHARMM36 [**?**]	0	1.0 12.	400:100	18647	419	298	200	200	[70]
POPC	CHARMM36 [**?**]	0	0	256	8704	0	300	300	250	[71]
POPC:POPE (1:1)	CHARMM36 [**?**]	0	0	128	8704	0	300	300	250	[72]
POPC	Slipid [**?**]	0.11	0	500	25000	48	310	500	100	[73]
POPC:POPG (7:3)	Slipid [**?**]	?	0	?	?	?	310	500	100	[**?**] 13.
POPC	Berger [**?**] 14.	0	0	256	10240	0	300	300	200	[74]
POPC:POPE (1:1)	Berger [**?**] 15.	0	0	128	11008	0	300	300	200	[75]
POPC:DOPE (1:1)	Berger [**?**] 16.	0	0	128	10240	0	300	300	200	[76]
DOPC	Berger [**?**] 17.	0	0	256	11008	0	300	300	200	[77]
DOPC:DOPE (1:1)	Berger [**?**] 18.	0	0	128	11008	0	300	300	200	[78]

[a]Number of lipid molecules with largest mole fraction
[b]Number of water molecules
[c]Number of additional cations
[d]Simulation temperature
[e]Total simulation time
[f]Time used for analysis
[g]Reference for simulation files

19.Data for POPC:POPG mixtures by listed by Antonio Peon is missing from this table

20.We need citations for the force fields.

RESULTS AND DISCUSSION

Headgroup and glycerol backbone order parameters of POPE and POPG from ^{13}C NMR

Absolute values of the headgroup and glycerol backbone order parameters from PE and PG lipids are measured previously using ^{2}H NMR [8, 11, 79, 80]. Because also the order parameter signs bear essential information about the lipid structures [13, 81], we measured the magnitudes and signs of POPE and POPG C–H bond headgroup and glycerol backbone order parameter in liquid phase using the 2D-RPDLF and S-DROSS experiments, as described previously [14, 20, 21]. For POPE, the glycerol backbone and α-carbon peaks in INEPT spectra were assigned based on previously measured POPC spectra [20] and the β-carbon peak was assigned based on ^{13}C chemical shift table for amines available at `https://www.chem.wisc.edu/areas/reich/nmr/c13-data/cdata.htm` (Fig. S1). For POPG, the glycerol backbone peaks in INEPT spectra were assigned based on previously measured POPC spectra [20], while α and γ-carbon peaks **21.How were these assigned?** (Fig. S2). The numerical value of the β-carbon order parameter could not be determined, because its peak overlapped with the g_2 peak from glycerol backbone in POPG. However, the order parameter of β-carbon is expected to be clearly smaller than for g_2 based on previous ^{2}H NMR measurements [8, 11, 80]. Therefore, the beginning of the S-DROSS curve gives the sign for g_2 order parameter and end for β (Fig. S2 (E)). This is confirmed with SIMPSON calculations using negative value for g_2 and positive value for β order parameter (Fig. S3). The POPE experiments were recorded at 310 K and POPG experiments at 298 K, where the bilayers are in the liquid disordered phase [82]. **22.Details to be checked by Tiago.**

As discussed previously for PC and PS headgroups [14, 81], also the headgroup and glycerol backbone order parameters of PE and PG are essentially independent of acyl chain composition, and therefore manifest mainly headgroup chemistry (Fig. 1). The glycerol backbone order parameters are similar for all the lipids, although they move slightly toward positive values (closer to zero) in the order PC $<$ PE $<$ PS $<$ PG. Also the headgroup order parameters of PC lipids are close PE, althought the latter gives systematically slightly more positive values (Fig. 1). The α-carbon order parameter of PG is similar to PE and PG, while the positive value of β-carbon is distinct from the other lipids. Notably, this difference was not observed in previous ^{2}H NMR experiments, because absolute value of β-carbon order parameter is similar in PG, PE and PC lipids and the order parameter signs were not measured [8, 11, 80].

In conclusion, the order parameter experiments suggest that the glycerol backbone conformations in all lipids and the headgroup conformations in PC and PE lipids are relatively similar, while PS and PG headgropus exhibit distinct conformational sampling. The details of sampled conformation are difficult to deduce from order parameters only, but the distinct headgroup order parameters of PS lipids are previously related to the more rigid structure of the headgroup [12, 14, 83].

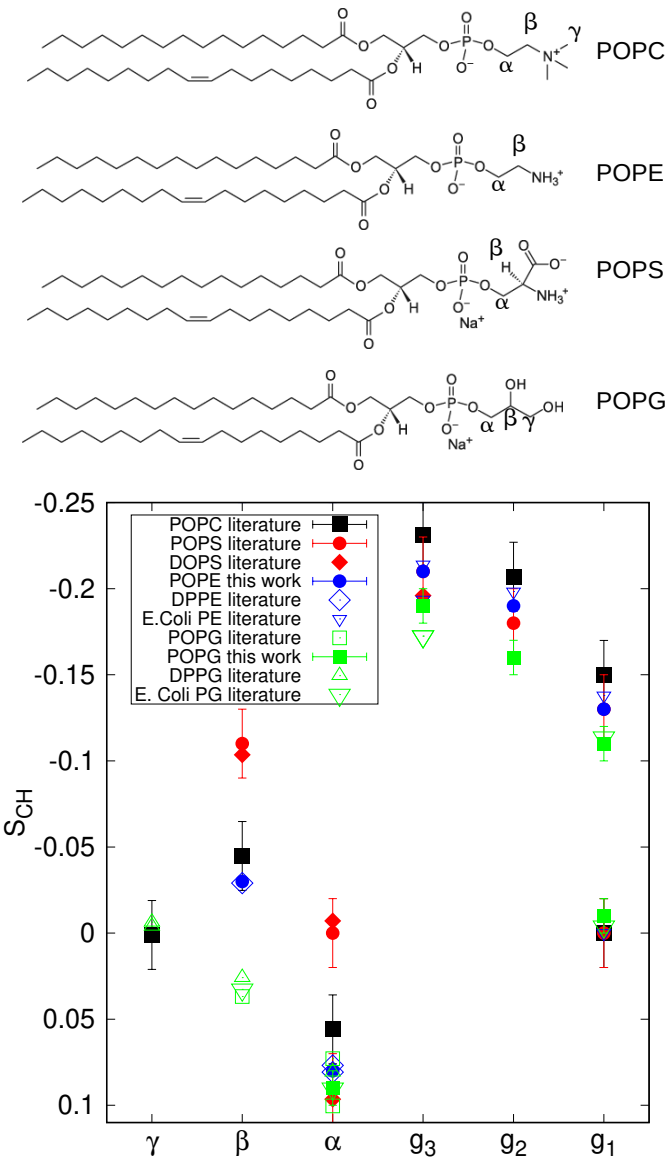

FIG. 1: (top) Chemical structure of different lipids. (bottom) Headgroup and glycerol backbone order parameters from different experiments in lamellar liquid disordered phase. The values and signs for POPE (310 K) and POPG (298 K) measured in this work, and for POPS (298 K) [14] and POPC (300 K) [20, 21] previously using ^{13}C NMR. The literature values for DOPS with 0.1M of NaCl (303 K) [83], POPG with 10nM PIPES (298 K) [80], DPPG with 10mM PIPES and 100mM NaCl (314 K) [11], DPPE (341 K) [79], E.coliPE and E.coliPG (310 K) [8] are measured using ^{2}H NMR. The signs from ^{13}C NMR are used also for the literature values.

23.The bottom figure could be clarified as Fig. 2 in the NMRlipids IVps paper.

Headgroup and glycerol backbone of POPE and POPG in MD simulations

Headgroup and glycerol backbone order parameters of PE and PG lipids show wide variation between different force fields and none of the force fields reproduce all values within experimental error bars. (Figs. 2 and 3), as observed previously also for PC and PS lipids [13, 14]. The poor performance of headgroup order parameters in Berger model can be probably explained by ring like structures seen in Fig. 6 in Ref. 84, which is a typical feature for Berger based lipid force fields containing explicit hydrogen atoms in the head group [85–87]. The poor performance of glycerol backbone of Slipids simulations is systemically observed also for other lipids in previous studies [13, 14]. **24.Should we comment more the relative quality of different force fields and/or make the subjective force field ranking figures?**

Without further discussion about poorly performing force fields, we focus on more detailed analysis of CHARMM36 simulations, which give the best overall agreement with experiments for the headgroup and glycerol backbone order parameters of all PC, PS, PG and PE lipids in this and our previous studies [13, 14]. Even thought many order parameters in CHARMM36 simulations are not within the experimental error bars, it seems to capture the essential differences between different headroups. In previous study, CHARMM36 predicted the more negative β-carbon order parameter and larger forking of the α-carbon in PS headgroup than in PC [14]. In this work, the PE headgroup order parameters are similar to the PC [13] and β-carbon order parameters is positive in PG headgroup, while negative values observed in other lipids. Therefore, we use CHARMM36 simulations to analyze the structural differences between headgroups (Fig. 4). **25.The structures are already in Fig. 4, but we need also the dihedral distributions to finish the discussion.**

26.Maybe we should analyze also some other structural features, at least P-N angles.

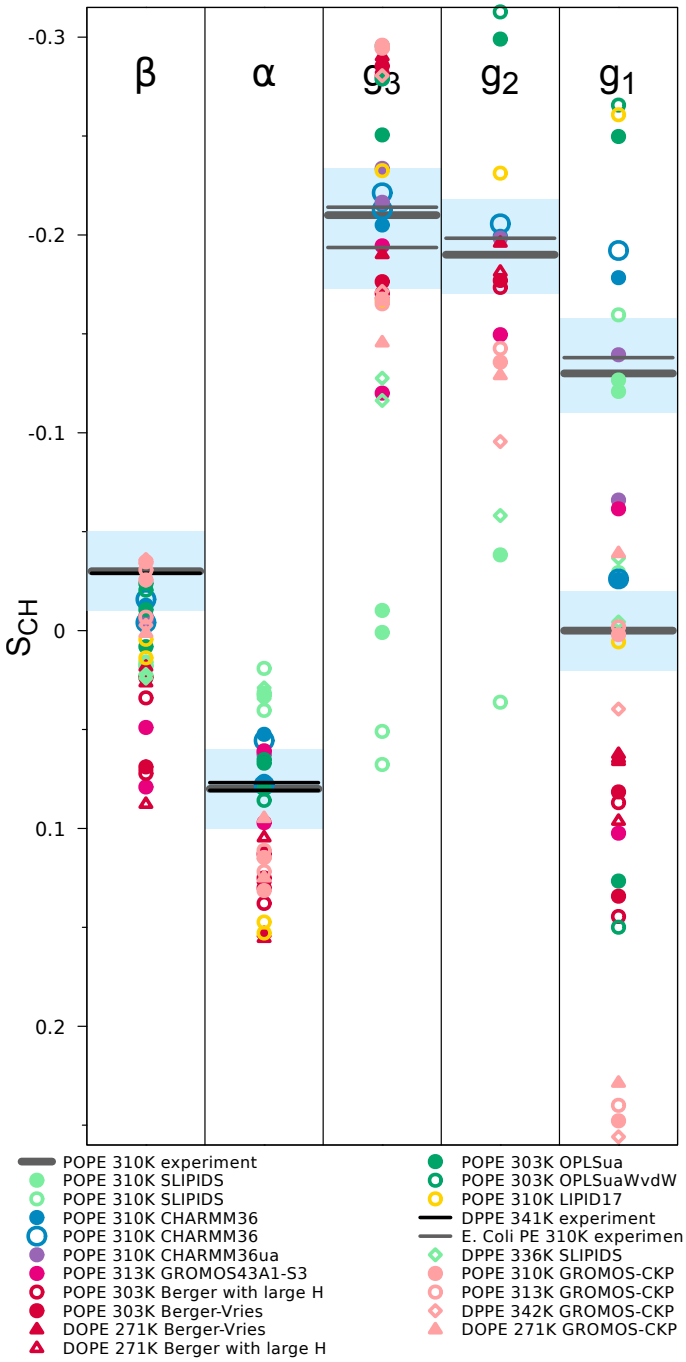

FIG. 2: The headgroup and glycerol backbone order parameters of PE lipids from experiments (POPE and signs this work, DPPE from Ref. 79 and E.coliPE from Ref. 8) and simulations with different force fields.

27.This should be clarified as in NMRlipidsI and error bars should be added. Probably larger error bars for united atom models based on the report by Fuchs et al.

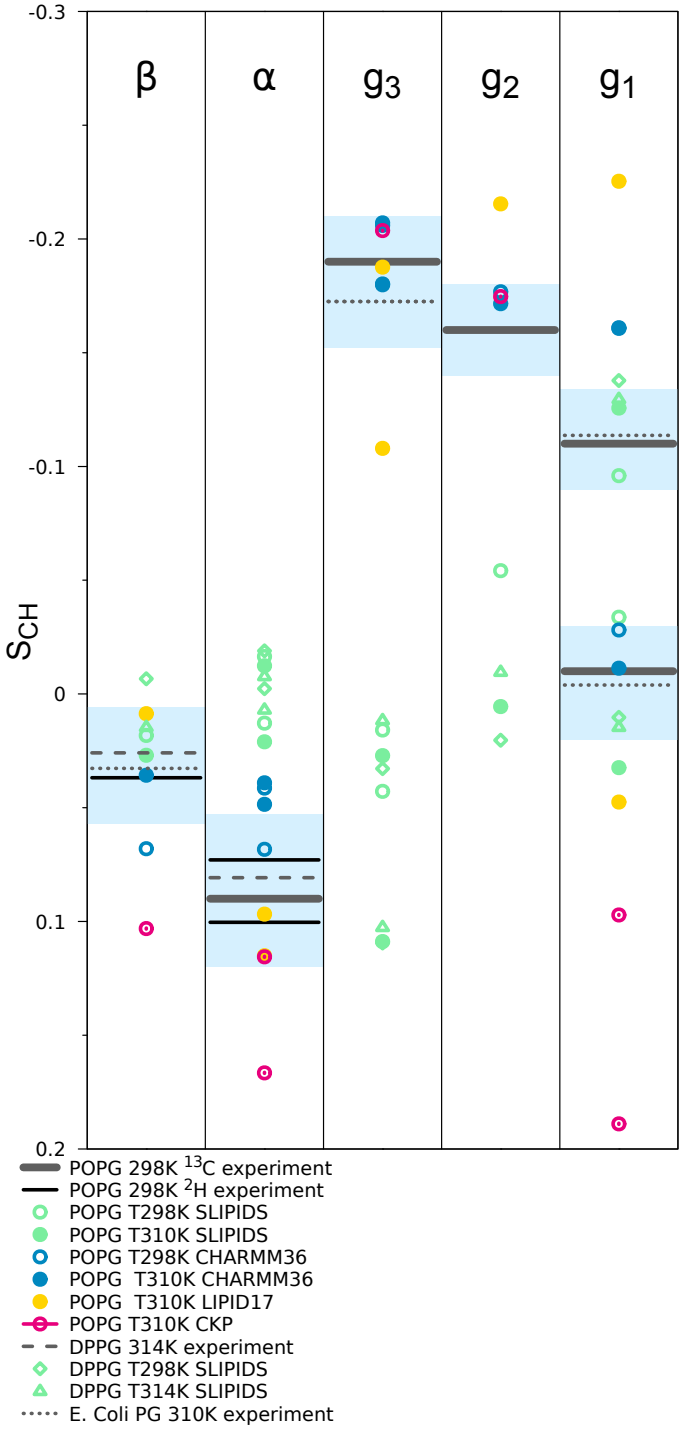

FIG. 3: The headgroup and glycerol backbone order parameters of PG lipids from experiments (POPG and signs from this work and from Ref. 80, DPPG with 100mM NaCl from Ref. 11,and E.Coli PG results from Ref. 8). and simulations with different force fields.

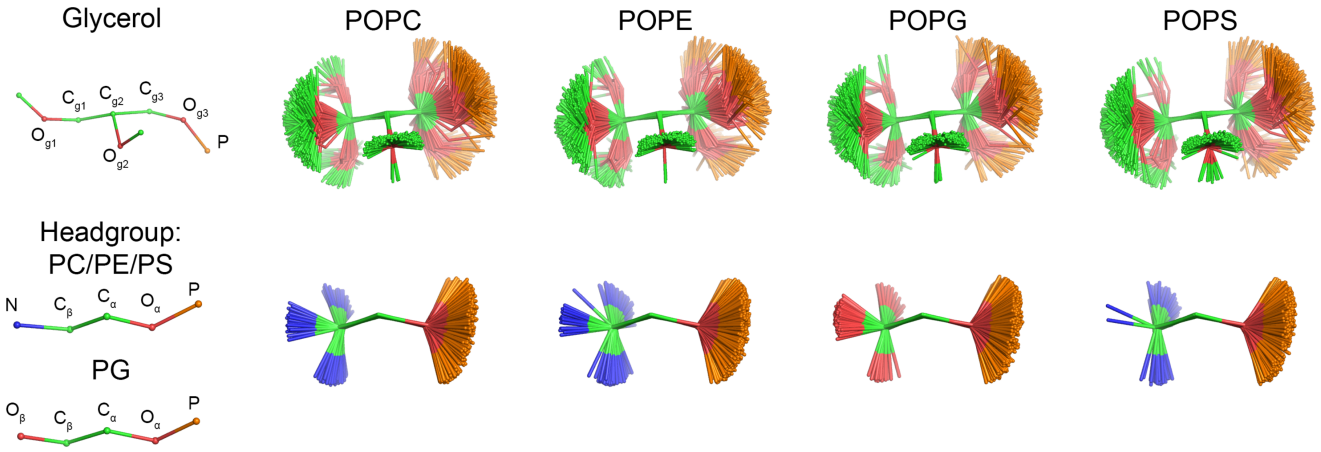

FIG. 4: Overlayed snapshots from CHARMM36 simulations of different lipids which give the best agreement with experiments.

PC headgroup interactions with PE and PG

In experiments, the PC headgroup order parameters increase with the addition of negatively charged PG or PS lipids, but are not affected by the addition of zwitterionic PE and SM lipids or cholesterol (Fig. 5). This can be explained by the electrometer concept, which suggests that the headgroup dipole tilts more parallel to the membrane plane upon addition of negative charge to the membrane [9, 89, 90]. The response of PC headgroup order parameters to PE by the tested CHARMM36 and Berger-OPLS force fields, although CHARMM36 slightly overestimates the changes (Fig. 5). The good performance of Berger-OPLS simulations is notable because the response of headgroup order parameters to cholesterol was significantly overestimated by the Berger/Höltje force field in our previous work [13]. None of the force fields fully reproduces the PC headgroup order parameter response to the increasing amount of PG, which may be related to the counterion binding affinity (see also the next section) [14]. In all force fields except Slipids, the order parameters of different hydrogens attached to the α-carbon are responsing differently when mixed with PE or PG lipids **28.Maybe we should figure out what is the reason for this?.**

29.Maybe we should analyze the P-N vector angle from different simulations?.

For β-carbon order parameter in PG headgroup, experiments report mild increase [88] or no change [80] upon addition of PC lipids (Fig. 6). Simulations with all the tested force fields give only very small changes also for the α-carbon order parameter (Figs. S4 and 6). Therefore, the simulations are generally in line with experiments, suggesting that the interactions with PC do not essentially effect the PG headgroup structure. This suggests that the interactions between PG and PC headgroups are captured better in simulations than for PS headgroup, where all the force fieds significantly overestimated the structural response of PS headgroup to the interactions with PC lipids [90].

30.This is text by P. Fuchs, copied from the blog.

Area results in nm^2, the error is $<=$ 0.003 nm^2

- pure POPC

CHARMM36: 0.624

Berger : 0.649

- POPC/POPE 50:50

CHARMM36 : POPC 0.609, POPE 0.557

Berger-hacked: POPC 0.637, POPE 0.632

—

One can see that CHARMM 36 predicts a drop in the area on going from pure POPC to POPC/POPE 50:50. This means that POPC pack tightly to POPE. In contrast, the values for Berger are not that changed. The POPE value predicted by CHARMM 36 (in the mixture POPC/POPE 50:50) is much smaller than that predicted by Berger.

——-

The experimental acyl chain order parameters for POPE [91] seem larger than reported for POPC [20], which supports the more condensed PE bilayer. This is interesting, but to avoid the overexapansion of the manuscript, it is probably better to keep the focus in headgroups and ion binding also in this manuscript.

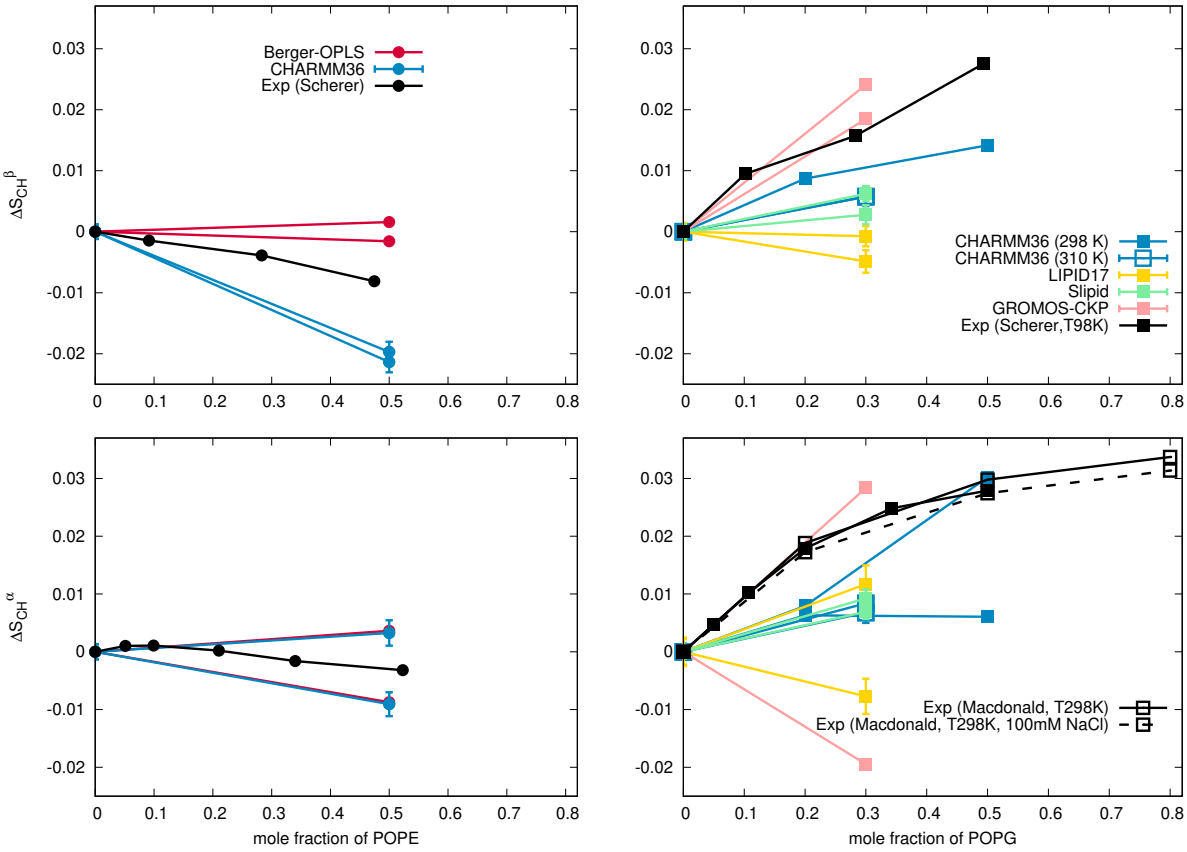

FIG. 5: Modulation of POPC headgroup order parameters with increasing amount of POPE (left) and POPG (right) in bilayer from experiments [9, 88] and simulations with different force fields. Signs are determined as discussed in [13, 81].

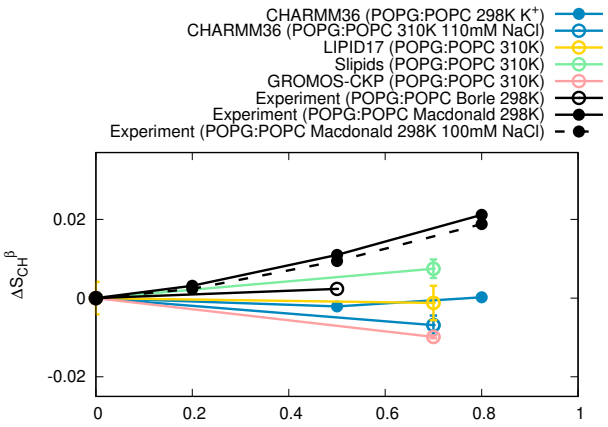

FIG. 6: Modulation of PG lipid headgroup order parameters with the increasing amount of PC in lipid bilayer from experiments [80, 88] and simulations with different force fields.

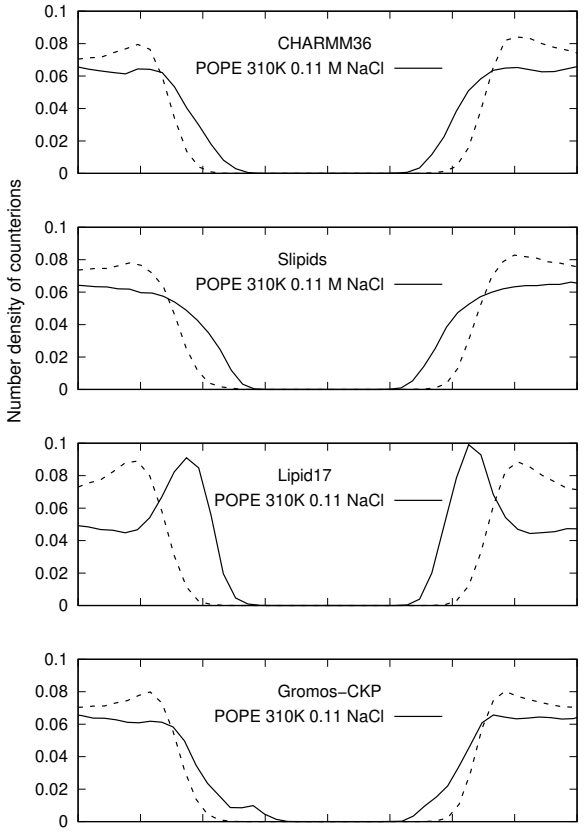

FIG. 7: Sodium (solid line) and choride ion density profiles along membrane normal from different simulations with PE lipids.

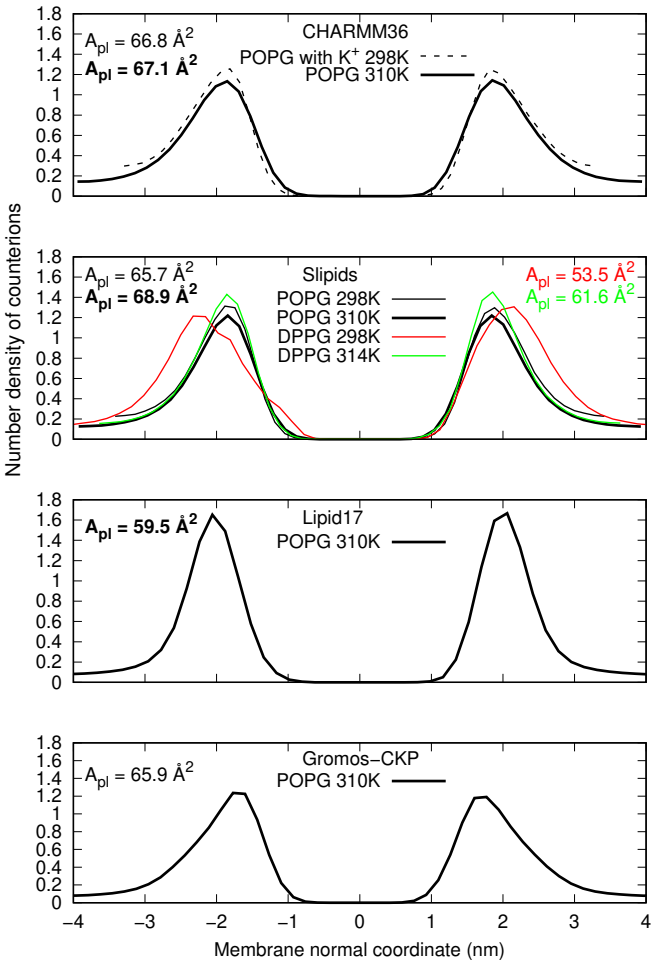

FIG. 8: Counterion densities and area per lipids from simulations with PG lipids. Experimental area for POPG at 303 K is 66.1 Å^2 and 67 Å^2 for DPPC at 323 K [92].

Sodium binding to PE and PG lipid bilayers

Sodium binding affinity to PE lipids has not been measured experimentally, but large differences to PC would be surprising. The sodium binding affinity to POPE depends on the used force field (Fig. 7), but lesser extend than reported previously for PC [15]. Because some simulation and ion parameters are not identical with the previous work [15] **31.This should be finished once we have the simulation details**, we compare POPE results to the POPC simulations ran with identical parameters (Fig. S5). In Lipid17 with the strongest sodium binding affinity to POPE, the binding affinity is approximately similar to POPC. Slipids and CHARMM36 exhibit slightly, and GROMOS-CKP substantially weaker binding to POPE than to POPC. Assuming that the binding to POPE would be similar than to POPC, the sodium binding affinity to POPE is potentially realistic in CHARMM36, Slipids, and GROMOS-CKP simulations here, but substantially overestimated in Lipid17 simulation.

Simulations with PG lipids give similar dependence on force field as observed in POPE simulations: Lipid 17 simulations exhibits stronger counter-ion binding affinity to pure POPG bilayer than CHARMM36, Slipids, and GROMOS-CKP simulations, which are roughly similar (Fig. 8). Lipid17 also exhibits less increase in POPC headgroup order parameters upon addition of POPG than other simulations (Fig. 5), and lower area per molecule (59.5 Å^2) than in experiments (66.1 Å^2). In our previous study about PS lipids [90], such behaviour was related to the overestimated counterions binding and shielding the electrostatic repulsion between PG headgroups in bilayers.Even though the area per lipid in CHARMM36, Slipids, and GROMOS-CKP simulations is in good agreement with experiments (Fig. 8), the experimental increase in POPC headgroup order parameters upon addition of POPG are not fully reproduced (Fig. 5). Therefore we conclude that the counter-ion binding affinity is overestimated in Lipid17 simulations, while the other simulations are more realistic, but slight overbinding cannot be excluded.

Cation binding to PE and PG lipid bilayers

The headgroup order parameters of PC lipids can used to measure ion binding affinity to lipid bilayers, because their magnitude is linearly proportional to the amount of bound charge in bilayer according to the molecular electrometer concept [15, 89]. The molecular electrometer concept can be used also for bilayers containing PC lipids mixed with charged lipids [14, 80, 88, 93]. The electrometer concept has been very useful in evaluating ion binding affinity in simulations against experiments, because the headgroup order parameter changes as a function of ion concentration can be directly compared with experiments [14–16].

Calcium binding affinity to PC and PS lipid bilayers was not correctly described by any of the standard MD simulation forced fields [14, 15], while recently introduced force field with electronic continuum correction (ECC) performed better [16]. The decrease of α-carbon order parameter of PC lipids in PC:PG mixtures as a function of calcium concentration is close to experiments CHARMM36 simulations (Fig. 9), but the decrease of β-carbon order parameter seems to be overestimated. However, the β-carbon order parameter was not actually measured from these samples, but they are calculated from empirical relation $\Delta S_\beta = 0.43 \Delta S_\alpha$ [94]. The result is similar to the $\sim$200 ns simulations with PC lipids in previous work [15]. However, when simulation was continued for μs, the binding affinity substantially increased and interpretation was that calcium overbinds to PC lipid in CHARMM36. Therefore, the conclusion seems to be similar here, although the new NBfix parameters may complicate the situation **32.The status of NBfix parameters in these simulations should be checked.**.

The β-carbon order parameter of PG exhibits a rapid decrease with small $CaCl_2$ concentrations and a more modest decrease with larger concentrations in experiments [80] (Fig. **??**). The rapid decrease with $CaCl_2$ is observed but overestimated in CHARMM36 simulation with POPC:POPG 1:1 mixture, but not in 4:1 mixture **33.This is little bit weird, should be checked.**.

34.We need PC:PG simulations with $CaCl_2$ from different force fields to finish the discussion.

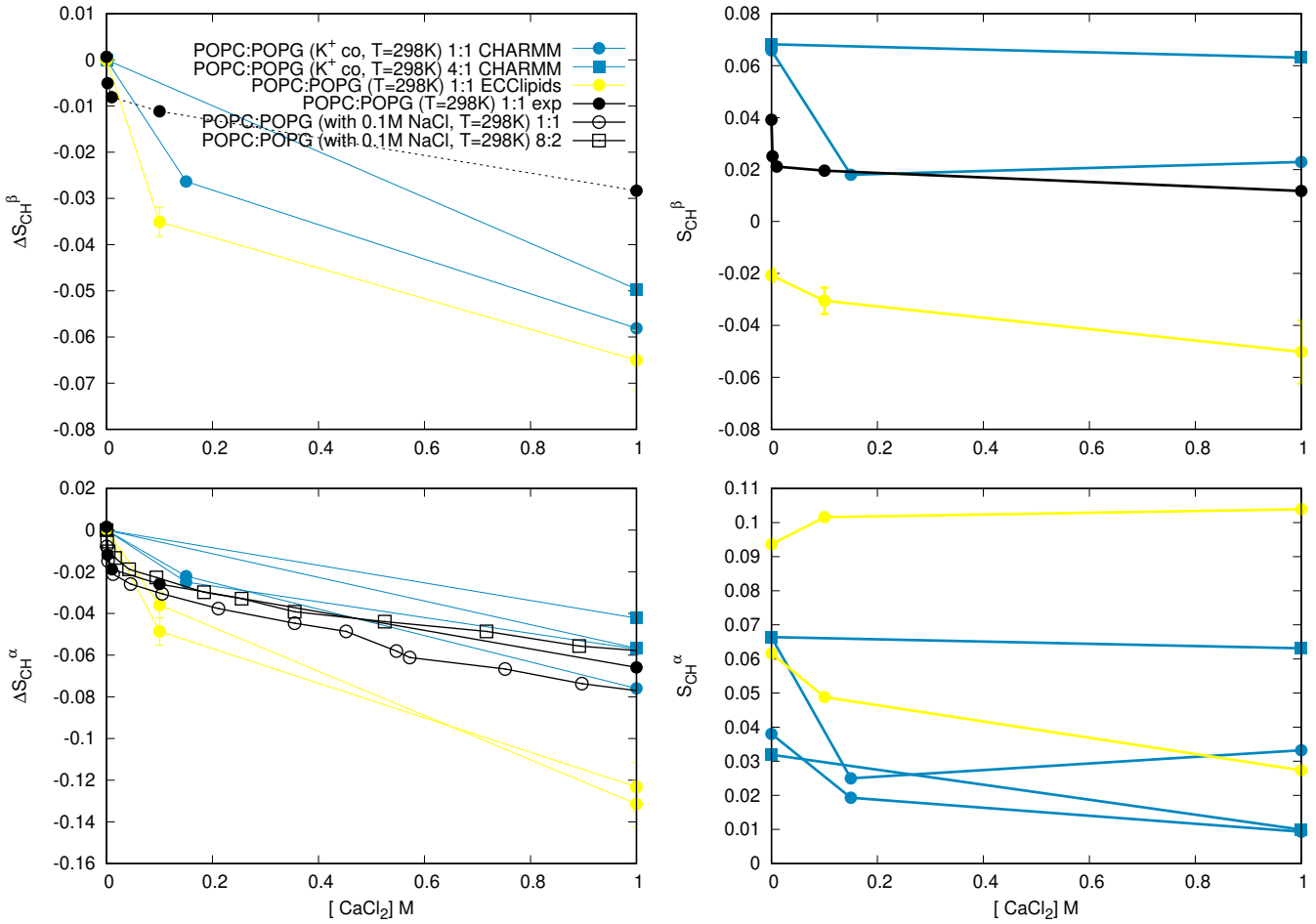

FIG. 9: (left) The headgroup order parameters of PC from PC:PG mixtures as a function $CaCl_2$ concentration from experiments [80, 88] and CHARMM36 simulations. Note that beta order parameter is calculated from empirical relation $\Delta S_\beta = 0.43\Delta S_\alpha$ [94], not actually measured. (right) The headgroup order parameters of PG from PC:PG mixtures as a function $CaCl_2$ concentration from experiments [80] and CHARMM36 simulations.

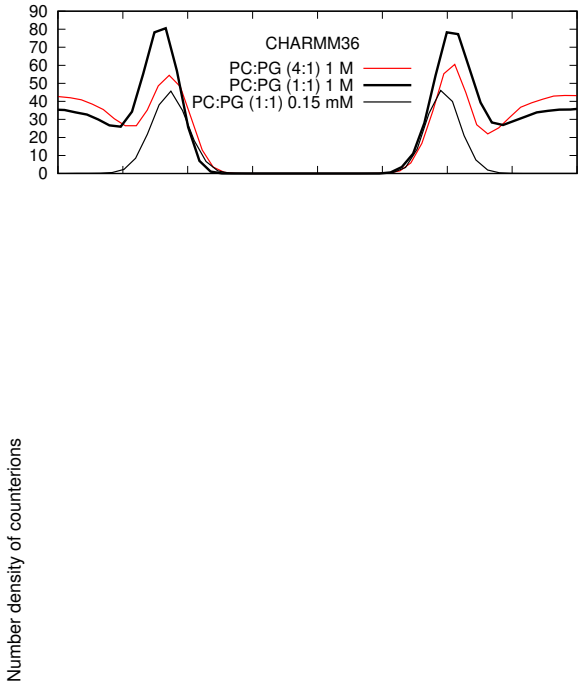

FIG. 10: Calcium ion density profiles along membrane normal from different simulations with PG lipids.

CONCLUSIONS

SUPPLEMENTARY INFORMATION

* samuli.ollila@helsinki.fi

[1] C. Sohlenkamp and O. Geiger, FEMS Microbiology Reviews **40**, 133 (2015).

[2] J. E. Vance, Traffic **16**, 1 (2015).

[3] E. Calzada, O. Onguka, and S. M. Claypool (Academic Press, 2016), vol. 321 of *International Review of Cell and Molecular Biology*, pp. 29 – 88.

[4] D. Patel and S. N. Witt, Oxidative Medicine and Cellular Longevity **2017**, 4829180 (2017).

[5] S. Furse, Journal of Chemical Biology **10**, 1 (2017).

[6] P. Hariharan, E. Tikhonova, J. Medeiros-Silva, A. Jeucken, M. V. Bogdanov, W. Dowhan, J. F. Brouwers, M. Weingarth, and L. Guan, BMC Biology **16**, 85 (2018).

[7] P. L. Yeagle, Biochimica et Biophysica Acta (BBA) - Biomembranes **1838**, 1548 (2014), membrane Structure and Function: Relevance in the Cell's Physiology, Pathology and Therapy.

[8] H. U. Gally, G. Pluschke, P. Overath, and J. Seelig, Biochemistry **20**, 1826 (1981).

[9] P. Scherer and J. Seelig, EMBO J. **6** (1987).

[10] J. Seelig, Cell Biology International Reports **14**, 353 (1990), ISSN 0309-1651, URL http://www.sciencedirect.com/science/article/pii/030916519091204H.

[11] R. Wohlgemuth, N. Waespe-Sarcevic, and J. Seelig, Biochemistry **19**, 3315 (1980).

[12] G. Büldt and R. Wohlgemuth, The Journal of Membrane Biology **58**, 81 (1981), ISSN 1432-1424, URL http://dx.doi.org/10.1007/BF01870972.

[13] A. Botan, F. Favela-Rosales, P. F. J. Fuchs, M. Javanainen, M. Kanduč, W. Kulig, A. Lamberg, C. Loison, A. Lyubartsev, M. S. Miettinen, et al., J. Phys. Chem. B **119**, 15075 (2015).

[14] H. S. Antila, P. Buslaev, F. Favela-Rosales, T. Mendes Ferreira, I. Gushchin, M. Javanainen, B. Kav, J. J. Madsen, J. Melcr, M. S. Miettinen, et al., The Journal of Physical Chemistry B p. acs.jpcb.9b06091 (2019), ISSN 1520-6106.

[15] A. Catte, M. Girych, M. Javanainen, C. Loison, J. Melcr, M. S. Miettinen, L. Monticelli, J. Maatta, V. S. Oganesyan, O. H. S. Ollila, et al., Phys. Chem. Chem. Phys. **18**, 32560 (2016).

[16] J. Melcr, H. Martinez-Seara, R. Nencini, J. Kolafa, P. Jungwirth, and O. H. S. Ollila, The Journal of Physical Chemistry B **122**, 4546 (2018).

[17] J. Melcr, T. Ferreira, P. Jungwirth, and O. H. S. Ollila, *Improved cation binding to lipid bilayer with negatively charged pops by effective inclusion of electronic polarization*, submitted, URL https://github.com/ohsOllila/ecc_lipids/blob/master/Manuscript/manuscript.pdf.

[18] S. V. Dvinskikh, H. Zimmermann, A. Maliniak, and D. Sandstrom, J. Magn. Reson. **168**, 194 (2004).

[19] J. D. Gross, D. E. Warschawski, and R. G. Griffin, J. Am. Chem. Soc. **119**, 796 (1997).

[20] T. M. Ferreira, F. Coreta-Gomes, O. H. S. Ollila, M. J. Moreno, W. L. C. Vaz, and D. Topgaard, Phys. Chem. Chem. Phys. **15**, 1976 (2013).

[21] T. M. Ferreira, R. Sood, R. Bärenwald, G. Carlström, D. Topgaard, K. Saalwächter, P. K. J. Kinnunen, and O. H. S. Ollila, Langmuir **32**, 6524 (2016).

[22] N. Michaud-Agrawal, E. J. Denning, T. B. Woolf, and O. Beckstein, Journal of Computational Chemistry **32**, 2319 (2011), https://onlinelibrary.wiley.com/doi/pdf/10.1002/jcc.21787,

URL https://onlinelibrary.wiley.com/doi/abs/10.1002/jcc.21787.

[23] Richard J. Gowers, Max Linke, Jonathan Barnoud, Tyler J. E. Reddy, Manuel N. Melo, Sean L. Seyler, Jan Domański, David L. Dotson, Sébastien Buchoux, Ian M. Kenney, et al., in *Proceedings of the 15th Python in Science Conference*, edited by Sebastian Benthall and Scott Rostrup (2016), pp. 98 – 105.

[24] ohsOllila and et al., *Match github repository*, URL https://github.com/NMRLipids/MATCH.

[25] P. Fuchs and et al., *Buildh github repository*, URL https://github.com/patrickfuchs/buildH.

[26] T. J. Piggot, J. R. Allison, R. B. Sessions, and J. W. Essex, J. Chem. Theory Comput. **13**, 5683 (2017).

[27] M. Abraham, D. van der Spoel, E. Lindahl, B. Hess, and the GROMACS development team, *GROMACS user manual version 5.0.7* (2015), URL www.gromacs.org.

[28] M. Javanainen, *Simulation of a POPE bilayer at 310K with the CHARMM36 force field* (2019), URL https://doi.org/10.5281/zenodo.2641987.

[29] PEON, *CHARMM36 POPE Bilayer Simulation (Last 100 ns, 310 K)* (2019), URL https://doi.org/10.5281/zenodo.3237461.

[30] A. PEÓN, *CHARMM36 POPE Bilayer Simulation (Last 100 ns, 150 mM NaCl, 310 K)* (2019), URL https://doi.org/10.5281/zenodo.2577454.

[31] T. Piggot, *CHARMM36-UA POPE Simulations (versions 1 and 2) 310 K (NOTE: hexagonal membrane and POPE is called PEUA)* (2018), URL https://doi.org/10.5281/zenodo.1293774.

[32] J. P. M. Jämbeck and A. P. Lyubartsev, J. Chem. Theory Comput. **8**, 2938 (2012).

[33] F. Favela-Rosales, *MD simulation trajectory of a fully hydrated DPPE bilayer: SLIPIDS, Gromacs 5.0.4. 2017.* (2017), URL https://doi.org/10.5281/zenodo.495247.

[34] T. Piggot, *Slipids POPE Simulations (versions 1 and 2) 310 K (NOTE: hexagonal membrane)* (2018), URL https://doi.org/10.5281/zenodo.1293813.

[35] A. Peon, *SLIPID POPE Bilayer Simulation (Last 100 ns, 310 K)* (2019), URL https://doi.org/10.5281/zenodo.3231342.

[36] A. PEÓN, *SLIPID POPE Bilayer Simulation (Last 100 ns, 150 mM NaCl, 310 K)* (2019), URL https://doi.org/10.5281/zenodo.2578069.

[37] T. Piggot, *GROMOS-CKP DPPE Simulations (versions 1 and 2) 342 K* (2018), URL https://doi.org/10.5281/zenodo.1293957.

[38] T. Piggot, *GROMOS-CKP POPE Simulations (versions 1 and 2) 313 K* (2018), URL https://doi.org/10.5281/zenodo.1293932.

[39] A. PEON, *GROMOS POPE Bilayer Simulation (Last 100 ns, 310 K)* (2019), URL https://doi.org/10.5281/zenodo.3237754.

[40] A. PEÓN, *Gromos POPE Bilayer Simulation (Last 100 ns, 150 mM NaCl, 310 K)* (2019), URL https://doi.org/10.5281/zenodo.2574491.

[41] T. Piggot, *GROMOS-CKP DOPE Simulations (versions 1 and 2) 271 K* (2018), URL https://doi.org/10.5281/zenodo.1293941.

[42] T. Piggot, *GROMOS 43A1-S3 POPE Simulations (versions 1 and 2) 313 K (NOTE: anisotropic pressure coupling)* (2018), URL https://doi.org/10.5281/zenodo.1293762.

[43] T. Piggot, *OPLS-UA POPE Simulations (versions 1 and 2) 303 K with vdW on H atoms* (2018), URL https://doi.org/10.5281/zenodo.1293853.

[44] T. Piggot, *Opls-ua pope simulations (versions 1 and 2) 303 k* (2018), URL https://doi.org/10.5281/zenodo.1293855.

[45] T. Piggot, *Berger POPE Simulations (versions 1 and 2) 303 K - de Vries repulsive H* (2018), URL https://doi.org/10.5281/zenodo.1293889.

[46] T. Piggot, *Berger POPE Simulations (versions 1 and 2) 303 K - larger repulsive H* (2018), URL https://doi.org/10.5281/zenodo.1293891.

[47] T. Piggot, *Berger DOPE Simulations (versions 1 and 2) 271 K - de Vries repulsive H* (2018), URL https://doi.org/10.5281/zenodo.1293928.

[48] T. Piggot, *Berger DOPE Simulations (versions 1 and 2) 271 K - larger repulsive H* (2018), URL https://doi.org/10.5281/zenodo.1293905.

[49] A. PEON, *LIPID17 POPE Bilayer Simulation (Last 100 ns, 310 K)* (2019), URL https://doi.org/10.5281/zenodo.3378970.

[50] A. PEÓN, *LIPID17 POPE Bilayer Simulation (Last 100 ns, 150 mM NaCl, 310 K)* (2019), URL https://doi.org/10.5281/zenodo.2577305.

[51] O. H. S. Ollila, *POPG lipid bilayer simulation at T298K ran with MODEL_CHARMM_GUI force field and Gromacs* (2017), URL https://doi.org/10.5281/zenodo.1011096.

[52] A. PEÓN, *CHARMM36 POPG Bilayer Simulation (Last 100 ns, 150 mM NaCl, 310 K)* (2019), URL https://doi.org/10.5281/zenodo.2573531.

[53] ANTONIO, *CHARMM36 POPG Bilayer Simulation (Last 100 ns, 310 K)* (2019), URL https://doi.org/10.5281/zenodo.3237463.

[54] J. P. M. Jämbeck and A. P. Lyubartsev, Phys. Chem. Chem. Phys. **15**, 4677 (2013).

[55] F. Favela-Rosales, *MD simulation trajectory of a fully hydrated POPG bilayer: SLIPIDS, Gromacs 5.0.4. 2017.* (2017), URL https://doi.org/10.5281/zenodo.546133.

[56] F. Favela-Rosales, *MD simulation trajectory of a fully hydrated DPPG bilayer @314K: SLIPIDS, Gromacs 5.0.4. 2017.* (2017), URL https://doi.org/10.5281/zenodo.546136.

[57] F. Favela-Rosales, *MD simulation trajectory of a fully hydrated DPPG bilayer @298K: SLIPIDS, Gromacs 5.0.4. 2017.* (2017), URL https://doi.org/10.5281/zenodo.546135.

[58] A. PEÓN, *SLIPID POPG Bilayer Simulation (Last 100 ns, 310 K)* (2019), URL https://doi.org/10.5281/zenodo.3364460.

[59] A. PEÓN, *SLIPID POPG Bilayer Simulation (Last 100 ns, 150 mM NaCl, 310 K)* (2019), URL https://doi.org/10.5281/zenodo.2633773.

[60] A. PEON, *LIPID17 POPG Bilayer Simulation (Last 100 ns, 310 K)* (2019), URL https://doi.org/10.5281/zenodo.3247659.

[61] A. PEÓN, *LIPID17 POPG Bilayer Simulation (Last 100 ns, 150 mM NaCl, 310 K)* (2019), URL https://doi.org/10.5281/zenodo.2573905.

[62] A. PEON, *GROMOS POPG Bilayer Simulation (Last 100 ns, 310 K)* (2019), URL https://doi.org/10.5281/zenodo.3266166.

[63] A. PEÓN, *Gromos POPG Bilayer Simulation (Last 100 ns, 150 mM NaCl, 310 K)* (2019), URL https://doi.org/10.5281/zenodo.3257649.

[64] A. Peón, *CHARMM36 POPC Bilayer Simulation (Last 100 ns, 150 mM NaCl, 310 K)* (2019), URL https://doi.org/10.5281/zenodo.2628335.

[65] A. PEÓN, *CHARMM36 POPC-POPG 7:3 Bilayer Simulation (Last 100 ns, 150 mM NaCl, 310 K)* (2019), URL https://doi.org/10.5281/zenodo.2580902.

[66] J. J. Madsen, *MD simulations of bilayers containing PC/PG mixtures and CaCl_2: 250POPC_250POPG_neutral* (2019), URL https://doi.org/10.5281/zenodo.3483787.

[67] J. J. Madsen, *MD simulations of bilayers containing PC/PG mixtures and CaCl_2: 250POPC_250POPG_0.15MCaCl_2* (2019), URL https://doi.org/10.5281/zenodo.3483789.

[68] J. J. Madsen, *MD simulations of bilayers containing PC/PG mixtures and CaCl_2: 250POPC_250POPG_1MCaCl_2* (2019), URL https://doi.org/10.5281/zenodo.3483793.

[69] J. J. Madsen, *MD simulations of bilayers containing PC/PG mixtures and CaCl_2: 400POPC_100POPG_neutral* (2019), URL https://doi.org/10.5281/zenodo.3483783.

[70] J. J. Madsen, *MD simulations of bilayers containing PC/PG mixtures and CaCl_2: 400POPC_100POPG_1MCaCl_2* (2019), URL https://doi.org/10.5281/zenodo.3483785.

[71] C. Papadopoulos and P. F. Fuchs, *CHARMM36 pure POPC MD simulation (300 K - 300ns - 1 bar)* (2018), URL https://doi.org/10.5281/zenodo.1306800.

[72] C. Papadopoulos and P. F. Fuchs, *CHARMM36 POPC/POPE (50%-50%) MD simulation (300 K - 300ns - 1 bar)* (2018), URL https://doi.org/10.5281/zenodo.1306821.

[73] A. PEÓN, *SLIPID POPC Bilayer Simulation (Last 100 ns, 150 mM NaCl, 310 K)* (2019), URL https://doi.org/10.5281/zenodo.2574689.

[74] B. Amélie and F. P. F.J., *Berger pure POPC MD simulation (300 K - 300ns - 1 bar)* (2018), URL https://doi.org/10.5281/zenodo.1402417.

[75] B. Amélie and F. P. F.J., *Berger POPC/POPE (50:50 ratio) MD simulation (300 K - 400ns - 1 bar)* (2018), URL https://doi.org/10.5281/zenodo.1402449.

[76] B. Amélie and F. P. F.J., *Berger POPC/DOPE (50:50 ratio) MD simulation (300 K - 300ns - 1 bar)* (2018), URL https://doi.org/10.5281/zenodo.1402441.

[77] B. Amélie and F. P. F.J., *Berger pure DOPC MD simulation (300 K - 300ns - 1 bar)* (2018), URL https://doi.org/10.5281/zenodo.1402411.

[78] B. Amélie and F. P. F.J., *Berger DOPC/DOPE (50:50 ratio) MD simulation (300 K - 300ns - 1 bar)* (2018), URL https://doi.org/10.5281/zenodo.1402437.

[79] J. Seelig and H. U. Gally, Biochemistry **15**, 5199 (1976).

[80] F. Borle and J. Seelig, Chemistry and Physics of Lipids **36**, 263 (1985).

[81] O. S. Ollila and G. Pabst, Biochimica et Biophysica Acta (BBA) - Biomembranes **1858**, 2512 (2016).

[82] D. Marsh, *Handbook of Lipid Bilayers, Second Edition* (RSC press, 2013).

[83] J. L. Browning and J. Seelig, Biochemistry **19**, 1262 (1980).

[84] P. Mukhopadhyay, L. Monticelli, and D. P. Tieleman, Biophysical Journal **86**, 1601 (2004).

[85] W. Zhao, T. Róg, A. A. Gurtovenko, I. Vattulainen, and M. Karttunen, Biochimie **90**, 930 (2008), ISSN 0300-9084, URL http://www.sciencedirect.com/science/article/pii/S0300908408000692.

[86] J. Hénin, W. Shinoda, and M. L. Klein, The Journal of Physical Chemistry B **113**, 6958 (2009).

[87] M. Dahlberg, A. Marini, B. Mennucci, and A. Maliniak, The Journal of Physical Chemistry A **114**, 4375 (2010).

[88] P. M. Macdonald and J. Seelig, Biochemistry **26**, 1231 (1987).

[89] J. Seelig, P. M. MacDonald, and P. G. Scherer, Biochemistry **26**, 7535 (1987).

[90] H. S. Antila, P. Buslaev, F. Favela-Rosales, T. Mendes Ferreira, I. Gushchin, M. Javanainen, B. Kav, J. J. Madsen, J. Melcr, M. S. Miettinen, et al., The Journal of Physical Chemistry B **0**, null (0), https://doi.org/10.1021/acs.jpcb.9b06091, URL https://doi.org/10.1021/acs.jpcb.9b06091.

[91] C. Paré and M. Lafleur, Biophysical Journal **74**, 899 (1998), ISSN 0006-3495, URL http://www.sciencedirect.com/science/article/pii/S0006349598740135.

[92] J. Pan, F. A. Heberle, S. Tristram-Nagle, M. Szymanski, M. Koepfinger, J. Katsaras, and N. Kučerka, Biochimica et Biophysica Acta (BBA) - Biomembranes **1818**, 2135 (2012).

[93] M. Roux and M. Bloom, Biochemistry **29**, 7077 (1990).

[94] H. Akutsu and J. Seelig, Biochemistry **20**, 7366 (1981).

ToDo

P.

1. Is this enough and correct, or should we repeat some methods from the NMRlipidsIVps paper? 1

2. BuildH program is now cited with a direct link to the GitHub repo. I think that a release to Zenodo would be nice in the final publication. 2

3. Maybe we should also shortly discuss here about the reasons for slight dependence of order parameter values on the method used to reconstruct hydrogens? 2

4. Ion parameters? 3

5. We need citations for the force fields. 3

6. Correct citation for CHARMM POPG 4

7. Ion parameters? 4

8. Ion parameters? 4

9. We need citations for the force fields. 4

10. Concentration calculated based in total amount of calcium ions. This may not be reasonable due to the lack of counterions. 4

11. Concentration calculated based in total amount of calcium ions. This may not be reasonable due to the lack of counterions. 4

12. Concentration calculated based in total amount of calcium ions. This may not be reasonable due to the lack of counterions. 4

13. Zenodo entry unclear. 4

14. This is probable not plain berger, correct force filed should be described. 4

15. This is probable not plain berger, correct force filed should be described. 4

16. This is probable not plain berger, correct force filed should be described. 4

17. This is probable not plain berger, correct force filed should be described. 4

18. This is probable not plain berger, correct force filed should be described. 4

19. Data for POPC:POPG mixtures by listed by Antonio Peon is missing from this table 4
20. We need citations for the force fields. 4
21. How were these assigned? 5
22. Details to be checked by Tiago 5
23. The bottom figure could be clarified as Fig. 2 in the NMRlipids IVps paper. 5
24. Should we comment more the relative quality of different force fields and/or make the subjective force field ranking figures? 6
25. The structures are already in Fig. 4, but we need also the dihedral distributions to finish the discussion . 6
26. Maybe we should analyze also some other structural features, at least P-N angles. 6
27. This should be clarified as in NMRlipidsI and error bars should be added. Probably larger error bars for united atom models based on the report by Fuchs et al. 6
28. Maybe we should figure out what is the reason for this? 9
29. Maybe we should analyze the P-N vector angle from different simulations? 9
30. This is text by P. Fuchs, copied from the blog. Area results in nm^2, the error is <= 0.003 nm^2
- pure POPC
CHARMM36: 0.624
Berger : 0.649
- POPC/POPE 50:50
CHARMM36 : POPC 0.609, POPE 0.557
Berger-hacked: POPC 0.637, POPE 0.632
——
One can see that CHARMM 36 predicts a drop in the area on going from pure POPC to POPC/POPE 50:50. This means that POPC pack tightly to POPE. In contrast, the values for Berger are not that changed. The POPE value predicted by CHARMM 36 (in the mixture POPC/POPE 50:50) is much smaller than that predicted by Berger.
——-
The experimental acyl chain order parameters for POPE [91] seem larger than reported for POPC [20], which supports the more condensed PE bilayer. This is interesting, but to avoid the overexapansion of the manuscript, it is probably better to keep the focus in headgroups and ion binding also in this manuscript. . . 9
31. This should be finished once we have the simulation details 12
32. The status of NBfix parameters in these simulations should be checked. 13
33. This is little bit weird, should be checked. 13
34. We need PC:PG simulations with $CaCl_2$ from different force fields to finish the discussion. 13